Single-blind detection, localization, and quantification of methane emissions using continuous path-integrated column measurements

Nathan Blume[1], Timothy G. Pernini[2], Jeremy T. Dobler[1],
T. Scott Zaccheo[2], Doug McGregor[1], Clay Bell[3,4]*

[1] Spectral Sensor Solutions, LLC, Fort Wayne, IN, 46818, USA
[2] Atmospheric and Environmental Research, Lexington, MA, 02421, USA
[3] Colorado State University, Fort Collins, Colorado, 80523, USA
[4] bpx energy, Denver, Colorado, 80202, USA

Correspondence to: Nathan Blume (nathan.blume@s-3llc.com)

Abstract. The GreenLITE™ emission monitoring system detected, located, and quantified methane (CH_4) emissions from a series of single-blind controlled releases with no prior knowledge of timing, locations, or release rates. System performance was evaluated against metrics defined in the Continuous Monitoring Protocol established by the Methane Emissions Technology Evaluation Center (METEC) at Colorado State University. This protocol allows more direct comparison of system performance between disparate measurement technologies. This experiment differs from similar tests where releases were conducted from equipment units at fixed locations at METEC by instead conducting releases at random locations anywhere within the central 0.18 km^2 of a 0.35 km^2 test site. The releases were much shorter in duration than those conducted in similar testing at METEC. GreenLITE™ detected 25 of 42 releases, which ranged in metered rate from 0.17 to 2.15 kg/h. The minimum detected emissions rate was 0.22 kg/h. GreenLITE™ demonstrated a 100% detection rate for releases ≥0.65 kg/h and average wind speed <5 m/s. The test site was subdivided into 20 boxes (109 × 83 m each), and the correct release box was identified in 9 cases, another 9 detections were localized to an adjacent box, and the remaining 7 were attributed elsewhere within the field. The average estimated emission rate bias was -6.1%. The 90% detection limit was 0.89 kg/h, while the wind-normalized detection limit was 0.44 (kg/h)/(m/s).

1   Introduction

Methane (CH_4) is the primary constituent of natural gas, a major source of heating and electricity generation around the world. CH_4 is also a potent greenhouse gas with a global warming potential 81-84 times that of carbon dioxide over a 20-year period (US EPA, 2023; IEA, 2021). The largest industrial sources of CH_4 in the United States are oil and natural gas systems, responsible for an estimated 29% of U.S. CH_4 emissions in 2020 (US EPA, 2022). Accurate characterization of CH_4 emissions in complex environments, such as many oil and gas facilities, is a challenging measurement problem due to limited access, potentially high emission rates creating safety concerns, a large number of potential emission locations, and high temporal variability in emissions (Riddick et al., 2022; Vaughn et al., 2018). In such environments, emissions can occur at many locations and at any time of day and year. Periodic leak detection and repair programs utilizing handheld optical gas imaging sensors, typically performed semi-annually or quarterly, may be effective at finding persistent leaks in expected locations (at equipment prone to leaking or failure), but they do not adequately address the problems of intermittent leaks not emitting at the time of the leak survey or leaks occurring in unexpected locations that may be omitted from the survey area (Lyon et al., 2015; Nathan et al., 2015; Zavala-Araiza et al., 2015). Periodic airborne leak surveys can have more complete spatial coverage but are generally less sensitive to small leaks, limited to midday periods when the boundary layer is well mixed, and expensive to operate (National Academies, 2018). Furthermore, leaks may persist for weeks or months before being detected by the next periodic survey, potentially resulting in significant total emissions of CH_4 and prohibiting the quantification of such emissions due to the uncertainty in duration. Continuous, wide-area monitoring over entire facilities has the potential to overcome these measurement gaps and to provide rapid detection of leaks with more accurate estimates of total time-integrated gas emissions from oil and gas production, distribution, and storage facilities.

In this single-blind study, a continuous monitoring approach was evaluated based on its ability to detect, locate, and quantify CH_4 emissions with no prior knowledge of emission location, time, rate, or duration. The GreenLITE™ gas concentration measurement system employs a continuous laser-absorption-spectroscopy-based, open-path, integrated column measurement in conjunction with an inverse dispersion model to locate and estimate CH_4 emission rates. While other open-path continuous monitoring methods require specific knowledge of potential leak locations to pre-position equipment such as reflective targets (Alden et al., 2019), the GreenLITE™ system utilized in this study is capable of identifying and localizing emissions from anywhere within the monitoring area. The ability of GreenLITE™ to detect, locate, and quantify CH_4 emissions was evaluated through the use of a set of performance metrics defined in the Continuous Monitoring Protocol (CMP) (CSU, 2020) developed under the Advancing Development of Emissions Detection (ADED) (CSU, 2022) program run by the Methane Emissions Technology Evaluation Center (METEC) at Colorado State University, Fort Collins, CO. By focusing on top-level metrics such as probability of detection and accuracy of localization and quantification rather than sensor-specific metrics such as concentration sensitivity and signal-to-noise ratio, the CMP aims to provide a means for regulatory agencies and oil and gas operators to directly compare the utility of different monitoring solutions.

Evaluation of other continuous monitoring solutions has been performed at the METEC facility, designed and built specifically for evaluation of CH_4 leak detection and quantification systems. The facility contains decommissioned oil and gas equipment representative of conventional and small non-conventional gas production facilities, namely wellheads, separation equipment, and small liquid storage tank batteries. While METEC provides realistic site topography, experimental design is still critical in evaluating the long-term expected performance of monitoring solutions at operational oil and gas facilities. For example, in prior experiments conducted at METEC in 2018 and described by Alden et al. (2019), for any given test, the pad containing the controlled emission was known to the sensing system operators, and the sensing system only needed to determine which equipment within the pad the emission source was located on. A total of 17 releases were performed, each lasting between 1.5 and 5.5 hours, with the release beginning and end times known by the sensing system operators. Emission rate and location within the pad were the sole blind aspects of these tests. The experiment provided only a single time window of about 4.25 hours during which no gas was released and false positive (FP) detections were possible. All other results provided were from known controlled releases, limiting assessment of the actual FP detection performance of the system being tested. More recent testing at METEC utilizing the CMP has addressed some of these methodological issues, with participating solutions fully blind, greater numbers of controlled releases, and more continuous operation allowing for greater opportunities for FP detections. (Bell et al., 2023).

The GreenLITE™ experiment detailed here applies the same CMP performance metrics utilized by METEC to a different test site while also attempting to avoid some of the shortcomings of similar monitoring technology evaluations. This study allowed for releases anywhere within 20 grid boxes covering a total area of over 0.18 km^2 at any time within a 12-hour daily window on any of 27 days. The longest release lasted one hour, and the average release was 22.8 minutes in duration. The GreenLITE™ system operated for more than 314 hours, with releases being conducted during only 5.1% of that time, leaving the rest of that time available for the possibility of FP detections. This experimental design allowed for a more representative

assessment of full-time continuous emissions monitoring capabilities over a monitoring area large enough to potentially include multiple operational oil and gas production facilities or represent a much larger single facility such as a refinery or tank farm (Lyon et al., 2016).

2 Materials and methods

2.1 Measurement system

GreenLITE™ is a laser absorption-based gas measurement system that consists of one or more optical transceiver units and some number of retroreflectors arranged such that a clear line of sight exists between each transceiver and each reflector. Backend processing and analytics convert measured optical depth values to gas concentrations in near-real time and generate 2-D distributions of CH_4 concentrations (Dobler et al., 2015; Dobler et al., 2017; Zaccheo et al., 2019). GreenLITE™ measurements are interfaced with an inverse dispersion model (IDM) to estimate CH_4 emission rates and locations. The measurement approach and emission retrieval scheme are described in detail in Pernini et al. (2022).

While GreenLITE™ may be used to measure the concentration over a single atmospheric path, the more common system configuration involves the transceiver scanning to multiple reflectors to measure an area. The transceiver optical head is scanned to sequentially point at each reflector for a period that typically spans 10 to 30 seconds depending on the application, measuring the path-integrated concentration of the target gas along the straight-line path ("chord") from the transceiver to the reflector. If two transceivers are arranged such that their measurement chords intersect one another (as seen in Fig. 1, for example), a 2-D reconstruction of the distribution of the gas concentration over an area that can span up to 25 km^2 can be obtained using a sparse tomographic approach (Dobler et al., 2015; Dobler et al., 2017).

Prior to this experiment, GreenLITE™ has previously been tested and deployed in several environments for CO_2 and CH_4 monitoring, including a 6-month study to monitor for CO_2 leaks from an underground carbon storage facility (Blakley et al., 2020), a 1-year study to monitor urban CO_2 emissions over central Paris, France (Dobler et al., 2017; Zaccheo et al., 2019; Lian et al., 2019), a 1-week evaluation of the CH_4 and CO_2 leak quantification ability of GreenLITE™ at an oil and gas facility (Watremez et al., 2018), and multiple campaigns monitoring fugitive CH_4 and CO_2 emissions from an oil sands open-pit mine and tailings pond (Pernini et al., 2022).

2.2 Measurement site

The experiment detailed in this paper was designed to simulate the area of a typical oil and gas storage tank farm. The chosen test site was a farm located in a rural area at the edge of a more suburban area. The site was mostly flat with few obstructions. While no known sources of CH_4 were present in the immediate vicinity of the test site, highways, shopping centers, housing developments, railroad tracks, and several active farms were present within a 2-km radius. While testing at a known experimental site such as METEC was considered, a site near the GreenLITE™ manufacturer was selected for these first blind tests based on experimental design consideration and time/cost constraints. Though the METEC facility more realistically

represents infrastructure at a typical oil and gas facility, GreenLITE™ is well suited for monitoring areas much larger than the ~0.03 km² METEC site. A GreenLITE™ deployment could monitor an area large enough to include multiple oil and gas production sites or a much larger single facility such as a refinery or tank farm. Furthermore, longer path lengths benefit the GreenLITE™ differential absorption measurement via higher signal-to-noise ratio due to the chosen wavelengths. The selected test site and methodology were reviewed by a METEC representative involved in the development of the ADED CMP. By performing the experiment on a much larger scale than what is possible at METEC, this work demonstrates that the ADED CMP is transferrable to any potential test location, enabling adaptation for a wider range of developing technologies. To the authors' knowledge, prior to this work, the CMP has not been applied to controlled release testing anywhere outside the METEC facility.

Detection, quantification, and localization performance metrics for the GreenLITE™ system (or any continuous monitoring sensor) may be expected to vary in different environments due to differences in area, topography, meteorology, and on-ground infrastructure, and the authors acknowledge that results from similar testing performed at an operational oil and gas facility would likely differ from the results of this work. The GreenLITE™ emissions measurement approach is robust in that measurement lines of sight and heights can be readily adapted to a given site by optimizing transceiver and reflector locations and heights for the site-specific application.

Meteorological data were provided by an onsite ATMOS 14 (measuring temperature, pressure, and relative humidity) and an ATMOS 22 (measuring wind speed and direction) from METER Group. See Appendix A for a more detailed description of the meteorological conditions experienced during testing.

2.3 System installation and setup

GreenLITE™ was set up at the farm test site as shown in Fig. 1. The layout included two GreenLITE™ transceivers and 29 retroreflectors arranged to provide 54 measurement chords covering an area of 0.35 km². Because of the flat site topography and lack of obstructions, all chord endpoints (transceiver optical heads and retroreflectors) were simply placed two meters above ground level, with optical heads mounted on custom pipe-frame structures and retroreflectors mounted on tripods. Measured chords ranged in length from 216 m to 817 m. The measurement area was subdivided into 44 potential emission location boxes. Releases could be conducted in any location other than the outermost boxes (for a total of 20 potential release boxes equaling 0.18 km²). The buffer boxes around the perimeter ensure that emissions within the site are not missed regardless of wind direction. While GreenLITE™ is able to monitor much larger areas (Dobler et al. 2017; Pernini et al., 2022), the area monitored in this experiment was primarily limited by property lines. Testing was performed in the time period from January to April, 2022, over a range of weather conditions. Local meteorological data were provided by an onsite weather station installed near transceiver T01 (green marker near lower left of Fig. 1).
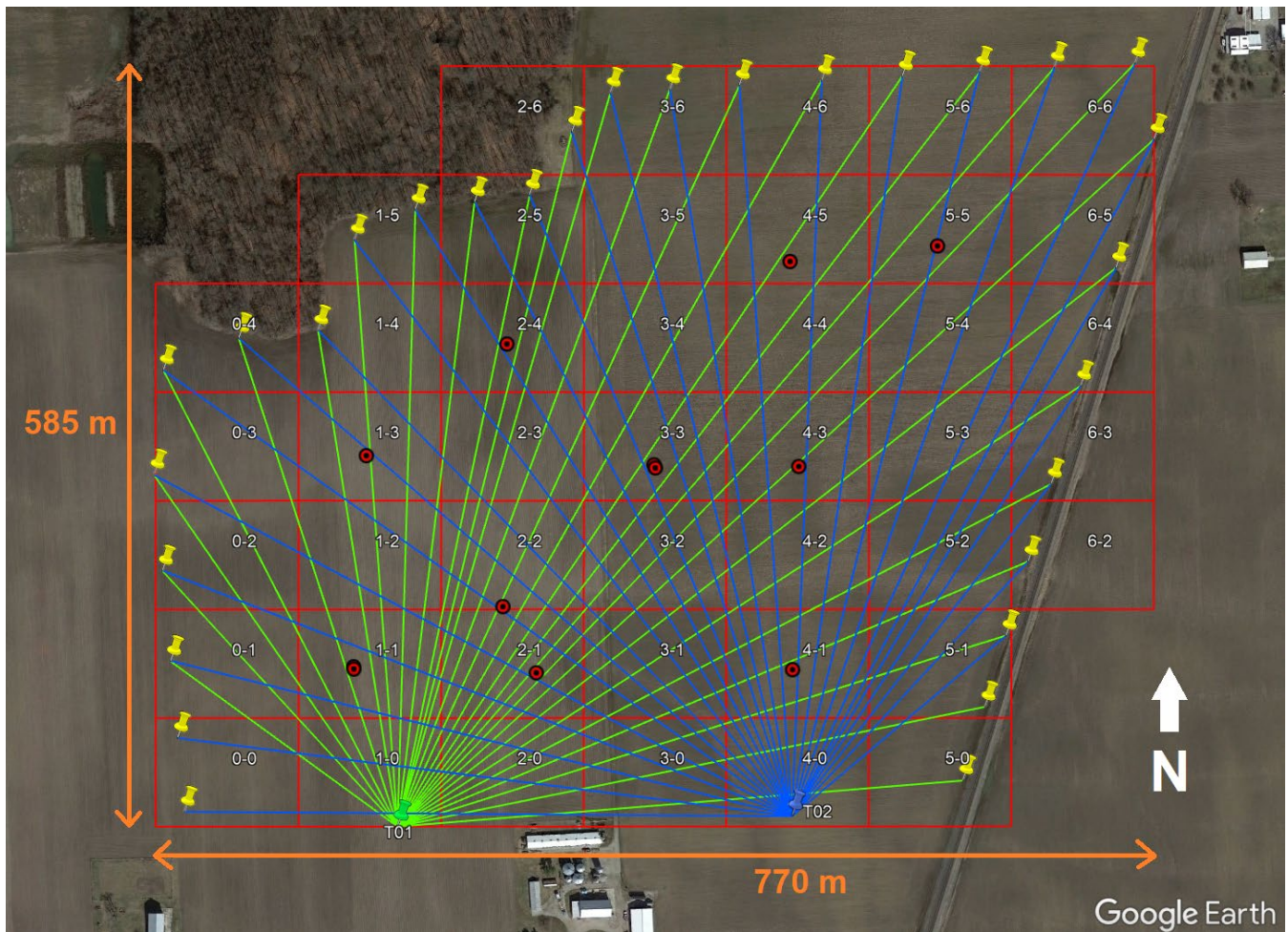
Figure 1: Layout of GreenLITE™ system at the test site. T01 and T02 are the two transceiver locations along the southern edge, yellow markers are the reflector locations, green lines are the chords measured by T01, and blue lines are the chords measured by T02. The red boxes are used as bounding boxes for computing emissions and providing an estimated location of the emission. Blind controlled release locations are marked with red and black bullseye symbols. Map Source: Google Earth © 2020

The system was installed in a non-permanent manner to avoid disruption to ongoing farming activities. Consequently, frequent ground freeze-thaw cycles experienced throughout the winter-spring testing period impacted optical alignment between the transceivers and reflectors. This was expected but unavoidable given the installation constraints. While GreenLITE™ is tolerant of very minor disturbances in optical alignment, larger disturbances result in the transmitted laser missing the reflector and causing insufficient optical power to be collected by the transceiver. Regular realignment was performed via the system's remote interface on all testing days, including both days when releases were performed and days when no releases were performed. Such realignment is not needed when GreenLITE™ is installed in a semi-permanent or permanent fashion, as was done in the deployments described by Dobler et al. (2017), Pernini et al. (2022) and Blakley et al. (2020).

2.4 Unblind release testing

A set of unblind releases was conducted in mid-January to evaluate the release procedure and verify expected performance. High-purity gas consisting of 99-99.5% pure CH_4 was used for all releases. Appendix B contains more information about the release system. A second round of unblind releases was conducted in late-January, allowing the detection sensitivity of the system to be coarsely evaluated and adjusted while providing guidance regarding the range of release rates that would be appropriate for the ensuing blind release tests. These unblind releases were performed at rates ranging from 0.17 to 2.15 kg/h. While storage tanks are known to be frequent emitters of CH_4 (Lyon et al., 2016), very little literature exists regarding true leak emission rates from oil and gas storage tanks due to the challenges associated with direct measurement of such leaks (Johnson et al., 2022). The release rates tested in this experiment are expected to be smaller than true emission rates from storage tanks and serve as an evaluation of the lower detection thresholds for the GreenLITE™ system. In theory, no upper detection limit exists for GreenLITE™, but quantification performance at higher emission rates may differ from that at the lower rates tested in this work.

Prior to conducting any blind releases, the test plan and test setup were audited onsite by a representative from METEC, whose recommendations were incorporated into the final test and execution.

2.5 Blind release testing

Recent evaluation of continuous monitoring systems at METEC included hundreds of individual releases, some lasting up to 8 hours, at emission rates up to 6.39 kg/h (Bell et al., 2023). In this study, releases were limited to rates ≤ 2.15 kg/h and durations ≤ 60 minutes due to limitations of the release system hardware and the prohibitive cost of large quantities of methane gas. Initial unblind test results indicated that high release rates were not needed to identify the minimum detection threshold and that short durations would provide ample information on detection thresholds to determine the 90% probability of detection emission rate. Blind releases ranged in duration from 12 minutes to one hour, with the average release lasting 22.8 minutes.

Personnel involved in this experiment were split into two groups: the test center team, responsible for planning, executing, and documenting the controlled releases; and the performer team, responsible for maintaining system operation and identifying, locating, quantifying, and reporting emission events. The test center team provided no information to the performer team regarding test days, times, durations, locations, or emission rates. This arrangement ensured that the performer team remained fully blind to the release schedule and details to allow for an unbiased assessment of the emission detection, localization, and quantification capabilities of GreenLITE™. For each release event, the test center team recorded all relevant information about the release. Releases occurred on six separate days dispersed over a six-week period containing 27 potential release days – 30 weekdays minus two days for power outage and one day for equipment maintenance. All releases occurred between 8:00 AM and 6:00 PM local time to ensure system alignment and to minimize the impact of frost heaving. Releases were conducted at 10 unique locations indicated in Fig. 1, with releases being repeated at two of those locations on different days.

A histogram of the releases as a function of release rate is provided in Fig. 2 (left). The right plot of Fig. 2 shows the number of GreenLITE™ scans as a function of release rate, which considers the duration of the release and the instrument scan rate. A complete scan producing concentration measurements on all 54 chords took approximately four minutes. More releases were performed at lower emission rates to improve confidence in the probability of detection evaluated at those rates, and higher emission rates were conducted for shorter release periods to limit gas consumption.
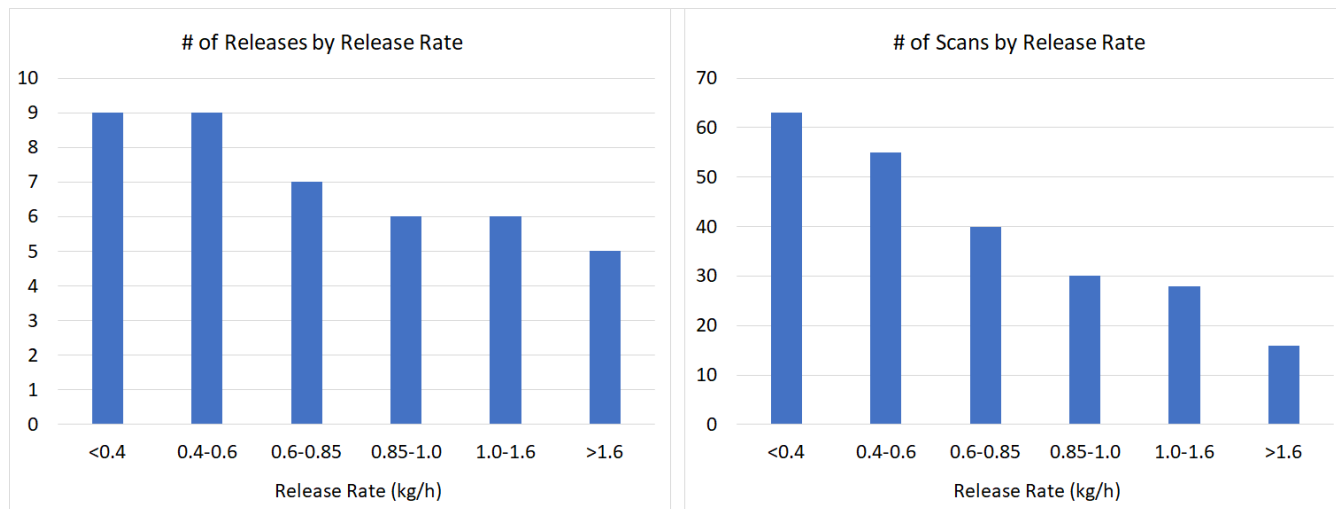
Figure 2: Distribution of the 42 releases as a function of release rate (left); Distribution of 4-minute GreenLITE™ scans as a function of release rate (accounts for release duration at each rate) (right).

If any emission events were detected, emission rates and locations were estimated for each detection or group of detections. All detections, localization and quantitative estimates were computed by the single-blind performer team at that time and reported for comparison to the test center team release record upon completion of blind testing.

2.6 Detection of emission events

The chord concentration measurements were passed through a detection algorithm to identify likely emission events. The median of all chord concentration measurements over a rolling time window was used to correct for natural variations in atmospheric background CH_4 concentration. Median chord-to-chord differences were removed through a flat-fielding correction prior to identification of chord concentration measurements exceeding the detection threshold. For each detection, the sample time, chord ID, and measured chord concentration were recorded in the detections file for that day.

2.7 Emission localization and quantification

The integrated column concentration measurements were combined with local wind information to create 2-D estimates of concentrations within the plane defined by the chords and their intersecting horizontal area using a sparse tomographic approach that minimizes the error between an analytical model of the field and the observed chord concentration values (Pernini et al., 2022). The 2-D concentration field is modelled as a set of rectangular subregions ("boxes").

The approach adopted in this study was to combine box retrieval data with a standard emissions modelling framework called Second-order Closure Integrated puff model with Chemistry (SCICHEM) [Chowdhury et al., 2015]. In this application, SCICHEM is used in an iterative scheme to provide emission estimates in the box sectors depicted with red lines in Fig. 1.

Detection times were used to determine which time periods to process for emissions estimation. Emission rates and locations were computed for each 10-minute time period in which an emission event had been identified by the detection algorithm. Since the concentration values associated with the 2-D box reconstructions are used in the iterative IDM emission retrieval scheme, emission locations were estimated to the fidelity of the red boxes shown in Fig. 1, with each emission event assigned to a numbered box. Emissions for each reconstruction box were computed, and the largest emission value in a non-edge box was provided as the estimated emission rate and the box as the emission location. The estimated emissions results, including the time window, emission rate, emission location, and average wind speed and direction over the time window, were recorded in the emissions file for that day. Emission rates were estimated in units of grams per hour (g/h) as per the CMP, but results are presented here in kg/h.

3   Results and discussion

Upon completion of all controlled releases, the reported detections and emissions results were compiled and compared to the test center release log data. Performance metrics were computed as defined in the CMP. Full results from each blind controlled release are provided in Appendix C.

3.1 Detection results

The primary CMP metrics related to detection are Probability of Detection (PD), False Positive Fraction (FPF), False Negative Fraction (FNF), and Detection Time (DT). PD is simply the number of true positive (TP) detections divided by the sum of the number of true positive and false negative (FN) detections. PD represents the fraction of emission events that were correctly identified.

The distribution of releases and detection as a function of release rate is shown in Fig. 3. A logistic regression is used to create a smooth, continuous PD curve from the discrete data samples, while a bootstrapping technique provides an indication of uncertainty in the result if experiments were repeated. Fig. 4 shows bootstrapped logistic-regression PD curves based on all detections from each release. This approach considers the number of releases at a given rate and the length of the releases. The bootstrapping technique envelopes the expected detection performance of the system under test and is performed by randomly selecting N detection samples out of N actual detections (with replacement) prior to performing the logistical regression. This process is repeated 100 times to build the grey curves seen in the left panel of Fig. 4, and the blue curve is the logistic regression fit to the estimated emissions.
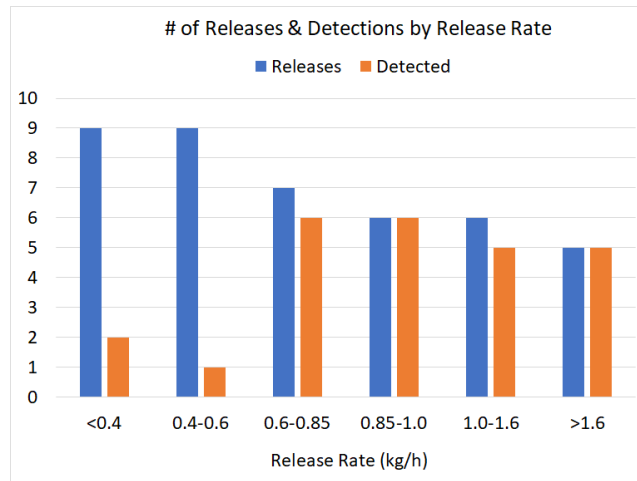
Figure 3: Distribution of total (blue) and detected (orange) releases as a function of release rate.
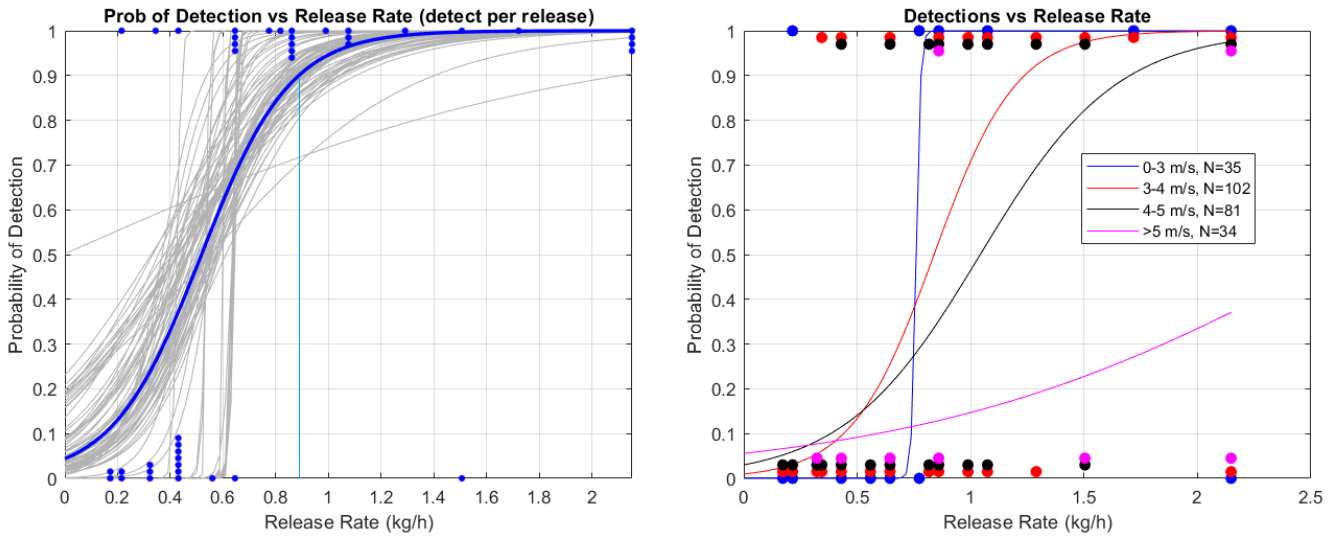

Figure 4: Probability-of-detection curves (blue: fit to data, grey: bootstrapping iterations) as a function of release rate (left); Probability of detection versus release rate and binned by wind speed (right). The left plot shows a 90% detection limit of 0.89 kg/h.

250   The right panel of Fig. 4 shows the PD curves, binned by average wind speed during the release, using a logistic regression without bootstrapping of the data. Note that the binning was chosen due to the limited number of samples at lower and higher wind speeds. The right panel of Fig. 4 indicates that one of the primary drivers of uncertainty in the PD curve is wind speed. To evaluate this further, a logistic regression with bootstrapping was performed using the release rate normalized by wind speed, consistent with analysis by Bell et al. (2022) and Sherwin et al. (2021) in the evaluation of other remote sensing systems.

255   The result is illustrated in Fig. 5 and shows a narrower confidence interval seen as a tighter grouping of the 100 bootstrap results.
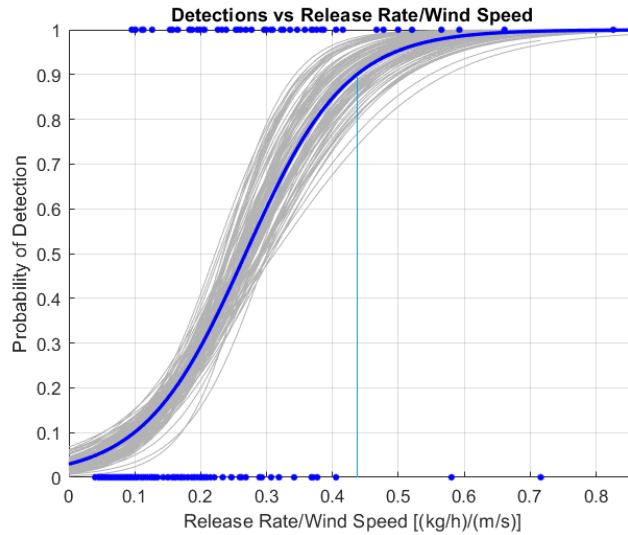
Figure 5: Logistic regression with bootstrapping using release rate normalized by wind speed, showing a 90% detection limit of 0.44 (kg/h)/(m/s).

Not captured in the previous figures is the number of FP detections and the FPF. FPF is the number of FP detections divided by the total number of reported detections. By definition, a FP detection is a reported detection that occurred at a time when no controlled release was being conducted. However, due to the uncontrolled nature of the test site and the fact that it is surrounded by a variety of potential CH_4 sources (e.g., homes, farms, forest, roads and highways, railroad tracks, shopping centers), a reported detection outside of a controlled release time may in fact be a detection of a true elevated CH_4 concentration from a source outside the monitored area. Appendix D contains details about two days on which off-site emissions sources were observed.

The total number of reported FP detections during the 6-week testing period was 31. These 31 FP detections occurred during a total non-release monitoring time of 298 hours and 17 minutes. The breakdown of FP detections between days with and without controlled releases (Table 1) shows no significant difference in FP rate between release and non-release days.

Table 1: Breakdown of FP detection frequency on days with and without controlled releases.

	# Days	# FP Detections	FP/Day
Days with Release	6	8	1.33
Days without Release	21	23	1.10

The CMP defines FPF as the number of FP detections divided by the total number of reported detections (FP + TP). The drawback to this definition is that the FPF is influenced as much by the number of releases and resulting TP detections as it is by the number of FP detections. A test consisting of many controlled releases and a short time period in which no releases are conducted will result in a lower FPF than one in which only a few releases are performed over a long period of operational time (as in the case of this experiment).

11

As defined by the CMP, the GreenLITE™ FPF for this single-blind test was 0.261 (31 FP / 119 total reported detections). Computing FPF in a manner similar to how FNF is computed may be more meaningful. FNF is defined as the number of FN detections divided by the number of controlled releases, which represents the fraction of controlled release periods not containing at least one TP detection. Alternatively, dividing the number of FP detections by the number of non-release periods represents the fraction of non-release periods containing at least one FP detection. We define this alternative metric as FPF′. A non-release period is defined as a period of time equal to the average duration of all controlled releases but containing no controlled release.

The average release duration for this experiment was 22.8 minutes. The total non-release time divided by the average release period yields 785 time periods of 22.8 minutes during which no controlled releases were conducted and results in a FPF′ of 0.039.

The FNF for this experiment is 0.40 for all release rates. Note that the FNF is influenced by the distribution of emission rates included in the experiments and is therefore more meaningful when considered as a function of release rate, as shown in Fig. 6. With the objective being to characterize the low-end sensitivity of the GreenLITE™ system, the vast majority of releases that did not produce detections were at relatively low rates (< 0.65 kg/h). The single FN detection at a rate greater than 0.65 kg/h was associated with a 16.7-minute release at 1.51 kg/h during which the average wind speed was 5.6 m/s (the highest of all controlled releases).
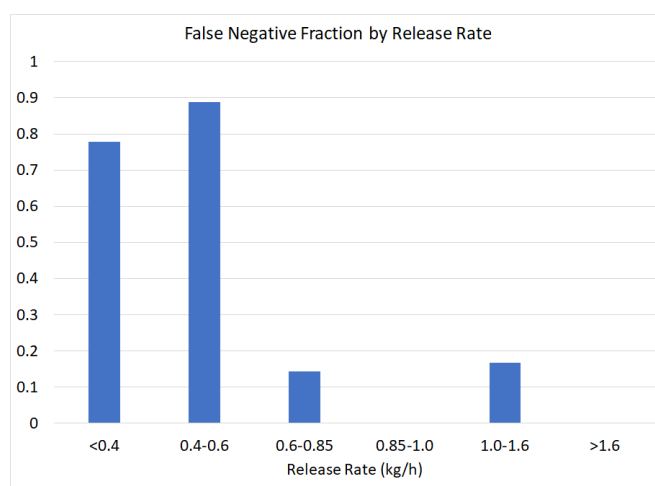

Figure 6: False negative fraction as a function of release rate.

Detection Time (DT) is defined as the elapsed time between the start of a release and the time when the release is first reported. DT values in this experiment ranged from 46 seconds to just under 23 minutes and exhibited an inverse relationship with metered release rate. Detailed DT results are given in Appendix E.

3.2 Emissions localization results

The primary metrics related to emission localization defined by the CMP are Localization Precision (LP) and Localization Accuracy (LA). The CMP requires that a detection report specify the emission location by identifying the Equipment Unit ID to which the emission is attributed. If an emission is believed to have originated from outside the testing area, it may be classified as Off Facility and excluded from the calculation of metrics. Because this experiment was performed in an agricultural setting and not on an operational or simulated oil and gas production facility, the test site included no equipment to which emissions could be attributed. Instead, each grid box (see Fig. 1) was assigned a unique identifier to represent the Equipment Unit ID for an emission event believed to have originated from within that area. The boxes immediately adjacent to a given box were defined as the Equipment Group. Each detected emission location was reported to the Unit level (i.e., to a specific box), and the reported locations were then compared to the true locations to compute the localization precision and accuracy metrics.

LP is simply a count of the number of detected releases that were identified to the correct Unit, Group, and Facility levels. Of the 25 detected blind controlled releases, 9 were correctly localized to the Unit level (box), 9 others to the Group level (adjacent box), and the remaining 7 to the Facility level (elsewhere within measurement footprint). A subset of the Group level detections included true release locations that were near the box boundary of the nearest downwind neighboring box. For these releases, wind likely carried the gas plume to a downwind measurement chord that passed through the neighboring box which was subsequently estimated to be the release box. In future work, both the proximity of the chord for which a detection occurred to respective box boundaries as well as wind speed/direction will be accounted for when localizing leaks, which should improve localization accuracy.

The LA metric represents the fraction of detections that were correctly identified at the Unit, Group, and Facility levels of precision. A detection correctly localized to the Unit level also counts as a detection at the correct Group and Facility levels. The GreenLITE™ LA metrics were also calculated with FP detections omitted, as was done by Bell et al. (2023), since the number of FP detections is a function of total monitoring time rather than the number of releases. The LA results are presented in Table 2.

Table 2: Localization Accuracy metrics as defined by the CMP and with FP detections omitted.

	Unit	Group	Facility
As Defined by CMP	0.161	0.321	0.446
With FP Detections Omitted	0.360	0.720	1.000

3.3 Emissions Rate Quantification Results

A secondary metric of the CMP is emission rate quantification accuracy. Emission rate quantification accuracy typically benefits from the averaging that longer release durations permit, whereas the short releases executed in this experiment presented a highly challenging scenario with little to no opportunity to average emissions estimates. The overall results of estimated emissions versus metered rates are provided in Fig. 7. Horizontal error bars represent the standard deviation of the

metered release rate as measured throughout each release. The figure depicts the overall fit between the estimated and metered emission rates for each release. These results indicate a bias of -6.1% from the linear fit with a fixed zero intercept. Relatively high variability is seen for release rates that were repeated multiple times, which may be due to a number of factors including wind conditions and proximity of release location to the nearest downwind measurement chord. Quantification error of individual rate estimates ranges from -89% to +263% of the metered release rate, with 80% of estimation errors falling between -67% and +67%.
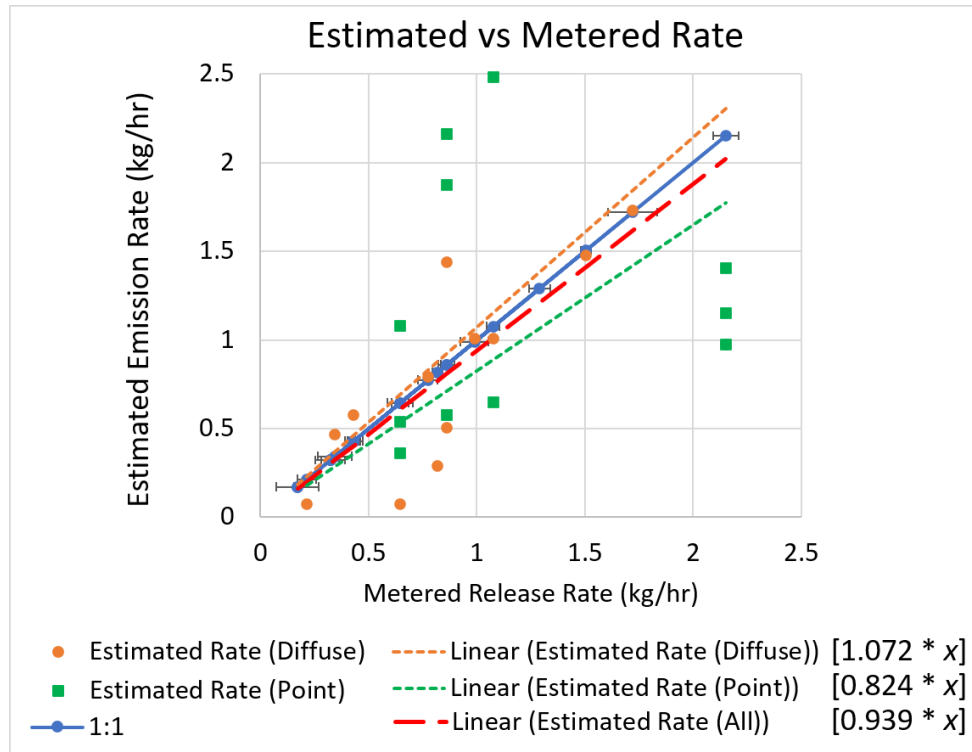

Figure 7: Estimated emission vs. metered release rates for all detections, separated by release method (point – green squares, diffuse – orange circles). This plot illustrates the fit relationships between metered and estimated rates for the entire set of detections achieved during this testing as well as for the detections separated by release method. Linear fits with no intercept indicate bias of +7.2% and -17.6% for diffuse (orange dotted line) and point (green dotted line) releases, respectively, while the fit to the entire dataset indicates a bias of -6.1% (red dashed line).

The quantification results presented here are representative only of the limited range of emission rates included in this experiment, which were selected to develop confidence in the PD curve as opposed to confidence in the quantification estimates over a much broader operational range. Quantification performance may be better or worse at higher emission rates, and further testing is required to determine the quantification accuracy of GreenLITE™ for larger emission events.

3.4 Operational factor

The last primary metric defined by the CMP is Operational Factor (OF), which represents the fraction of time a system is operational relative to the total planned testing time. The total planned testing time was 345.4 hours, while the operational time totaled 314.2 hours, for an OF of 0.910. Causes of down time included laser beam attenuation due to thick fog and heavy rain, failure of a component power supply, and operator error. This calculation does not include the two periods of time when power to the equipment was disrupted due to a local power outage.

4   Conclusions

4.1 Results summary and implications

The results from this single-blind study show that, with no prior knowledge of potential leak locations, rates, times, or durations, GreenLITE™ can detect CH_4 emissions as small as 0.22 kg/h and that, for the 22 controlled releases with average wind speeds <5 m/s, it demonstrated a 100% detection rate for leaks ≥ 0.65 kg/h. Of the 42 releases in total, 25 were detected as emission events. For localization, the correct release box (Unit) was determined for 9 of the detections, an adjacent box (Group) was identified in 9 of the detections, and the remaining 7 were localized elsewhere within the field (Facility). Quantification of the 25 detected emissions exhibited a bias of -6.1%. These results represent an important first step in demonstrating feasibility of the GreenLITE™ system to offer continuous monitoring of relatively large oil and gas facilities to identify, locate, and quantify CH_4 emission sources, including those from arbitrary locations at random times.

Additional testing to further assess the capabilities of GreenLITE™ for use in monitoring oil and gas facilities should include the presence of multiple emissions sources, allowed (known or expected) emission events, and higher emissions rates, as well as testing in a more relevant environment containing oil and gas equipment and infrastructure.

While the CMP metrics are a useful framework for providing a method to compare the key characteristics of continuous monitoring systems that are most of interest to oil and gas operators and regulators, our work illuminates some refinements that could be made to further increase the utility of the metrics. Limitations of the CMP methodology to perform classification of detections as TP or FP detections have been identified in other testing programs (Bell et al., 2023), suggesting a need to consider the application or use case of the continuous monitoring system under evaluation and to tailor the methodology as appropriate. Defining FPF such that it is not dependent on the number of controlled releases would allow more meaningful comparison between systems tested under very different experimental designs. One such solution would be to compute FPF as the number of FP detections reported per 24-hour period of system operation. A modified LA metric that does not utilize the Unit/Group/Facility classification method would provide more consistency across monitoring systems intended for different use cases. The experiment detailed here was intended to evaluate the ability of GreenLITE™ to detect, quantify, and localize leaks from oil and gas storage tanks rather than from well pads. Thus, an equipment Unit was defined to be much larger in size than it would have been if attempting to localize a leak to a specific valve or compressor. Determination of LA

using some distance-based measure would allow better comparison of results from testing performed at facilities of different

375   scales.

4.2 Potential future improvements

The GreenLITE™ emission detection algorithm can be modified to apply a temporal requirement such that multiple detection events must occur within a specified time window before a detection is reported. This change will result in a reduction in FP detections and increase confidence that reported detections are TP detections. Due to the relatively short duration of releases

380   included in this experiment, a quantitative analysis of the potential improvement was not conducted.

Emissions localization and quantification may be improved by more fully utilizing measured wind speed and direction as well as the proximity of measurement chords to box boundaries. For example, a localization constraint limiting possible predicted leak locations to boxes that fall on or upwind of detection chords may further improve localization performance. Emission localization and quantification accuracy may also be improved by using a Gaussian plume reconstruction approach

385   with the emission source modeled as a point emission in the IDM rather than the box reconstruction with area emission sources. This is supported by the quantification estimates separated by release type, shown in Fig. 7, which show better agreement between estimated rates for diffuse releases than for point releases using the box reconstructions.

16

Appendix A: Test conditions

Average temperatures during the test period ranged from -6° C in Jan/Feb to +15° C in April. Average wind speed for the test period was 3.2 m/s, with the prevailing wind out of the southwest and west, as shown in Fig. A1.
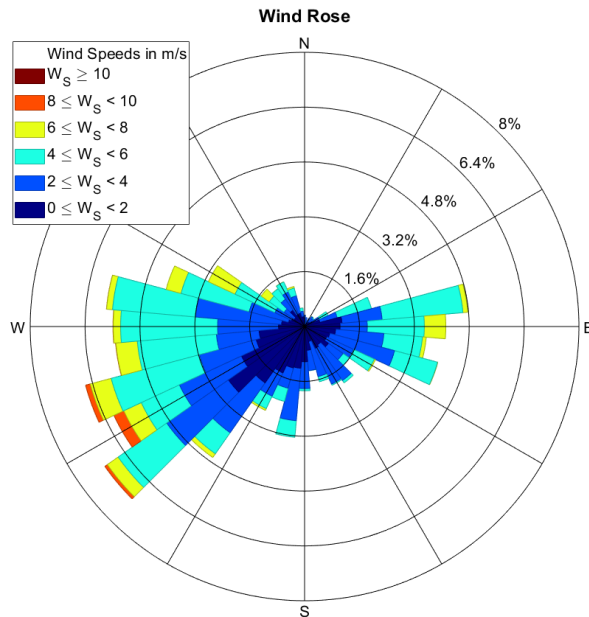

Figure A1: Wind rose depicting distribution of wind direction and speed during blind testing period (15 Mar – 26 Apr, 2022).

Appendix B: Controlled release system

The controlled release system consisted of a pressurized cylinder containing of 99-99.5% pure CH_4, a single-stage regulator, an Omega FMA-1609A mass flow meter (2.15 kg/h max), a computer with custom software for logging the flow meter output, a 15-meter vinyl hose, and a 3 m × 3 m PVC pipe diffuser (optionally attached for "diffuse source" releases). A diagram of the release system is shown in Fig. B1.
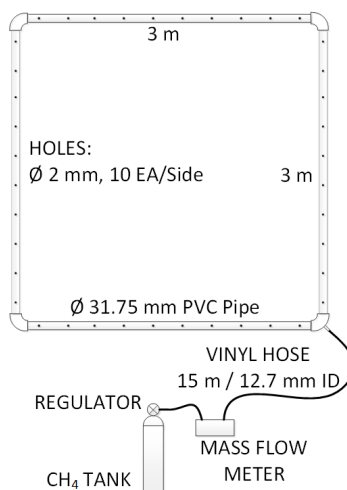
400

Figure B1: PVC disseminator assembly for producing diffuse gas releases with release setup. Point releases were produced directly from the vinyl hose without the PVC structure.

Appendix C: Controlled release results

Tables C1 and C2 contain results from the blind controlled release testing and related definitions for interpretation.

405   **Table C1: Definitions of columns in summary of results in Table C2.**

Parameter	Parameter Description
relID	first number is release location designator; second number is sequential release number at that location
det	binary value of a detection during the release (1 = detected, 0 = not detected)
relScans	number of sensor scans completed during release period
detScans	number of sensor scans resulting in detection during release period
relBox	grid box where release was conducted
emisBox	box identified by analytics as the emission location
locPrecision	Unit: emisBox equal to relBox;
	Group: emisBox adjacent to relBox;
	Facility: emisBox not equal or adjacent to relBox
relRate	metered release rate in grams per hour
emisRate	estimated emissions rate in grams per hour
quantAccAbs	emisRate minus relRate in grams per hour
quantAccRel	quantAccAbs divided by relRate
detTime	time between a detection and the last data point needed to establish that detection (HH:MM:SS)

18

Table C2: Results for all blind releases. Emission rate and location information are only present in the table for those releases which were positively detected. Releases with releaseID values beginning with digits less than 05 were unblind releases and are not presented in these results.

relID	det	relScans	detScans	relBox	emisBox	locPrecision	relRate	emisRate	quantAccAbs	quantAccRel	detTime
05-01	1	8	1	1-3	5-1	FACILITY	215.1	72	-143.1	-0.665	08:41:21
05-02	1	4	3	1-3	1-4	GROUP	1290.6	4680	3389.4	2.626	07:23:00
05-03	0	7	0	1-3			430.2	0	-430.2	-1	00:00:00
06-01	1	4	2	2-2	3-1	GROUP	860.4	576	-284.4	-0.331	03:58:50
06-02	1	3	2	2-2	2-2	UNIT	2151	1404	-747	-0.347	03:20:24
06-03	1	4	3	2-2	3-5	FACILITY	860.4	2160	1299.6	1.51	02:31:33
07-01	1	3	2	4-5	4-5	UNIT	2151	1152	-999	-0.464	09:02:58
07-02	1	3	3	4-5	4-5	UNIT	1720.8	1728	7.2	0.004	08:28:24
07-03	0	7	0	4-5			215.1	0	-215.1	-1	00:00:00
08-01	1	4	3	4-1	5-2	GROUP	860.4	1440	579.6	0.674	06:47:26
08-02	1	8	2	4-1	4-1	UNIT	430.2	576	145.8	0.339	05:09:42
08-03	1	4	4	4-1	5-2	GROUP	1075.5	2484	1408.5	1.31	04:14:53
09-01	1	8	5	1-1	1-1	UNIT	860.4	504	-356.4	-0.414	09:50:00
09-02	0	5	0	1-1			322.65	0	-322.7	-1	00:00:00
10-01	0	7	0	4-3			322.65	0	-322.7	-1	00:00:00
10-02	1	3	2	4-3	4-2	GROUP	2151	972	-1179	-0.548	05:49:00
10-03	1	4	1	4-3	5-1	FACILITY	645.3	540	-105.3	-0.163	05:10:10
10-04	1	5	4	4-3	4-3	UNIT	1075.5	648	-427.5	-0.397	04:07:52
11-01	0	3	0	2-4			172.08	0	-172.1	-1	00:00:00
11-02	1	5	1	2-4	1-4	GROUP	645.3	72	-573.3	-0.888	09:10:41
11-03	0	4	0	2-4			430.2	0	-430.2	-1	00:00:00
12-01	1	8	3	3-3	3-4	GROUP	344.16	468	123.8	0.36	07:45:44
12-02	1	6	3	3-3	3-3	UNIT	989.46	1008	18.5	0.019	06:56:15
13-01	0	7	0	2-1			430.2	0	-430.2	-1	00:00:00
13-02	1	7	1	2-1	4-5	FACILITY	645.3	1080	434.7	0.674	04:28:55
13-03	1	5	1	2-1	5-5	FACILITY	817.38	288	-529.4	-0.648	03:40:15
14-01	1	5	4	5-5	5-5	UNIT	774.36	792	17.6	0.023	10:35:26
14-02	1	7	1	5-5	5-5	UNIT	645.3	360	-285.3	-0.442	09:30:06
15-01	0	15	0	3-3			172.08	0	-172.1	-1	00:00:00
15-02	0	6	0	3-3			322.65	0	-322.7	-1	00:00:00
15-03	0	8	0	3-3			559.26	0	-559.3	-1	00:00:00
15-04	1	5	3	3-3	5-5	FACILITY	1075.5	1008	-67.5	-0.063	11:03:50
15-05	0	4	0	3-3			215.1	0	-215.1	-1	00:00:00
15-06	0	4	0	3-3			430.2	0	-430.2	-1	00:00:00
15-07	1	6	3	3-3	4-4	GROUP	1505.7	1476	-29.7	-0.02	08:27:57
15-08	0	7	0	3-3			430.2	0	-430.2	-1	00:00:00
15-09	0	7	0	3-3			645.3	0	-645.3	-1	00:00:00
16-01	0	6	0	1-1			430.2	0	-430.2	-1	00:00:00
16-02	1	4	3	1-1	1-4	FACILITY	860.4	1872	1011.6	1.176	04:21:17
16-03	1	4	2	1-1	2-1	GROUP	2151	972	-1179	-0.548	03:38:09
16-04	0	4	0	1-1			430.2	0	-430.2	-1	00:00:00
16-05	0	4	0	1-1			1505.7	0	-1505.7	-1	00:00:00

Appendix D: Detection of off-site emissions sources

On the morning of 17 March 2022, there were 105 detections in a span of about 80 minutes during which time no controlled releases were conducted. A nearby Picarro G2301 sampling ambient air located slightly south of the southern edge of the monitored area showed an elevated background CH_4 concentration. Fig. D1 shows the GreenLITE™ detections and the concentration measured by the Picarro.
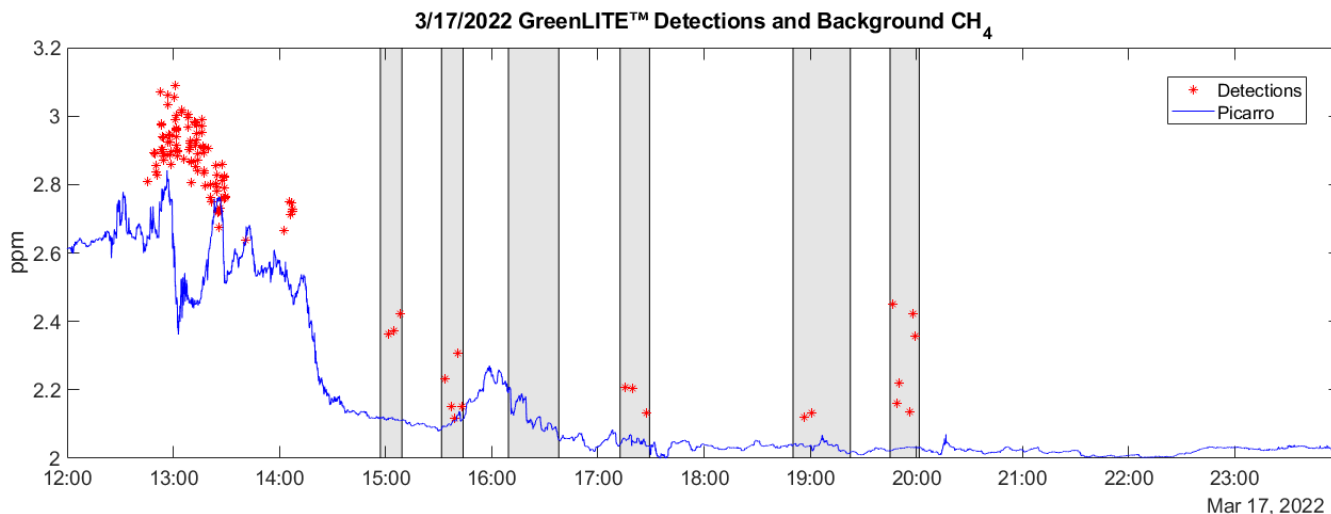

Figure D1: A large cluster of GreenLITE™ detections (red stars) coincides with elevated background concentration measured by a nearby Picarro G2301 (blue line, location indicated by black star near bottom of Fig. D2) on 17 March 2022.
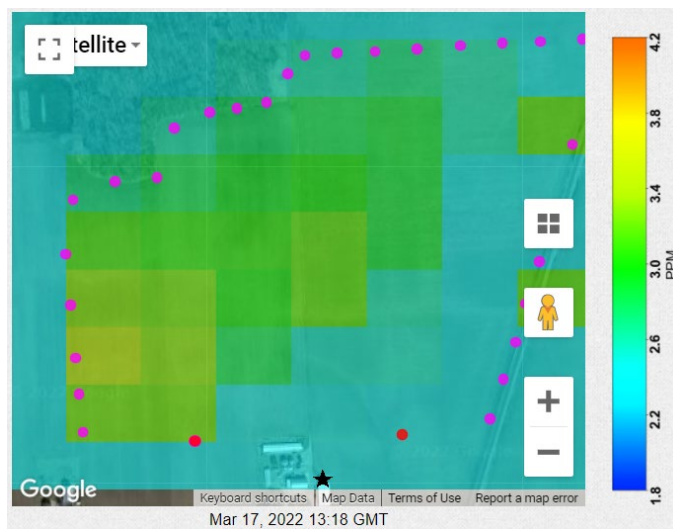
Figure D2: 2-D reconstruction of CH_4 emissions during period of frequently occurring detections showing evidence of an offsite source southwest of the monitored area. Wind direction at this time was from the southwest at 218°. The black star near the bottom indicates the location of the Picarro ambient CH_4 sensor. Map Source: Google Maps © 2022

The 2-D reconstruction of the concentration as measured by GreenLITE™ and shown in Fig. D2 indicates an offsite source
425   blowing into the monitored area. The wind direction during the time period in which the cluster of non-controlled-release
detections occurred ranged from 210 to 240 degrees (south-southwest to southwest). A very similar event occurred on March
21, with 93 detections occurring in 104 minutes. Because the detections in these time periods were caused by an outside source,
and because the CMP states that detections identified as "OFF_FACILITY" are not classified as FP detections, they have not
been counted as FP detections in these metrics or included in the calculation of FPF.

430   **Appendix E: Detection time results**

Figure E1 shows the DT as a function of release rate. As expected, DT trends toward shorter times as release rates increase.
At the time the test plan was audited by the METEC representative, the real-time detection algorithm was not fully
implemented. In following the audited test plan, DT results reported to EPA were generated with data analyzed for detections
at the end of each test day and ranged from 6 hours, 19 minutes to 11 hours, 4 minutes (equal to the elapsed time from the
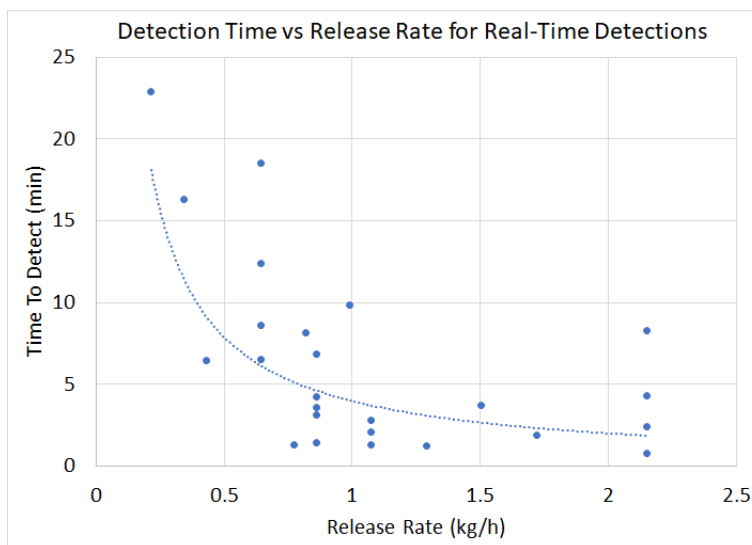435   chord measurement indicating a detection to the end of the daily collection period).

Figure E1: Detection times as a function of release rate using real-time detection algorithm, shown with power fit.

Code and data availability. Sample data sets and results corresponding to this study are available upon request from the
corresponding author.

440   *Author contributions.* JTD led this study. NB and JTD designed the experiment with input from CB. JTD and DM performed
the controlled releases. NB, TGP, and TSZ performed data analysis. CB provided an independent audit of the experimental

design and controlled release system as well as recommendations for statistical analysis methods. NB and TGP generated all manuscript figures. All authors reviewed and edited the manuscript.

References

455 Alden, C. B., Coburn, S. C., Wright, R. J., Baumann, E., Cossel, K., Perez, E., Hoenig, E., Prasad, K., Coddington, I., and Rieker, G. B.: Single-blind quantification of natural gas leaks from 1 km distance using frequency combs, Environ. Sci. Technol., 2019, 53(3), 2908-17, DOI: 10.1021/acs.est.8b06259.

Bell, C., Ilonze, C., Duggan, A., and Zimmerle, D.: Performance of continuous emission monitoring solutions under single-blind controlled testing protocol, Environ. Sci. Technol., 2023, 57(14), 5794-5805, DOI: 10.1021/acs.est.2c09235.

460 Bell, C., Rutherford, J., Brandt, A., Sherwin, E., Vaughn, T., and Zimmerle, D.: Single-blind determination of methane detection limits and quantification accuracy using aircraft-based LiDAR, Elementa: Science of the Anthropocene., 2022. 10, 00080, DOI: 10.1525/elementa.2022.00080.

Blakley, C., Carman, C., Korose, C., Luman, D., Zimmerman, J., Frish, M., Dobler, J., Blume, N., and Zaccheo, S.: Application of emerging monitoring techniques at the Illinois Basin – Decatur Project, Int. J. Greenh. Gas Con., 2020. 103, 103188,
465 DOI: 10.1016/j.ijggc.2020.103188.

Chowdhury, B., Karamchandani, P. K., Sykes, R. I., Henn, D. S., and Knipping, E.: Reactive puff model SCICHEM: Model enhancements and performance studies, Atmos. Environ., 2015. 117, 242–258, DOI: 10.1016/j.atmosenv.2015.07.012.

Colorado State University (CSU) Energy Institute, Advancing Development of Emissions Detection: https://energy.colostate.edu/metec/aded, last accessed: 12 Dec 2022.

470 Colorado State University (CSU) Energy Institute, METEC Controlled Test Protocol: Continuous Monitoring Emission Detection and Quantification, 2020: https://energy.colostate.edu/wp-content/uploads/sites/28/2021/03/Continuous-Monitoring-Protocol-R1.0.pdf, last accessed: 12 Dec 2022.

Dobler, J. T., Zaccheo, T. S., Blume, N., Braun, M., Botos, C., and Pernini, T. G.: Spatial mapping of greenhouse gases using laser absorption spectrometers at local scales of interest, Proc. SPIE 9645, Lidar Technologies, Techniques, and

475 Measurements for Atmospheric Remote Sensing XI, Toulouse, France, 2015. 96450K, DOI: 10.1117/12.2197713.

Dobler, J. T., Zaccheo, T. S., Pernini, T. G., Blume, N., Broquet, G., Vogel, F., Ramonet, M., Braun, M., Staufer, J., Ciais, P., and Botos, C.: Demonstration of spatial greenhouse gas mapping using laser absorption spectrometers on local scales, J. Appl. Remote Sens., 2017. 11, 014002, DOI: 10.1117/1.JRS.11.014002.

International Energy Agency (IEA), Methane Tracker 2021: https://www.iea.org/reports/methane-tracker-2021/methane-and-

480 climate-change, last accessed: 6 June 2023.

Johnson, D., Clark, N., Heltzel, R., Darzi, M., Footer, T. L., Herndon, S., and Thoma, E. D.: Methane emissions from oil and gas production sites and their storage tanks in West Virginia, Atmos. Environ.: X, 2022. 16, 100193, DOI: 10.1016/j.aeaoa.2022.100193.

Lian, J., Bréon, F.-M., Broquet, G., Zaccheo, T. S., Dobler, J., Ramonet, M., Staufer, J., Santaren, D., Xueref-Remy, I., and

485 Ciais, P.: Analysis of temporal and spatial variability of atmospheric CO2 concentration within Paris from the GreenLITE™ laser imaging experiment, Atmos. Chem. Phys., 2019. 19, 13809–13825, DOI: 10.5194/acp-19-13809-2019.

Lyon, D. R., Alvarez, R. A., Zavala-Araiza, D., Brandt, A. R., Jackson, R. B., and Hamburg, S.P.: Aerial surveys of elevated hydrocarbon emissions from oil and gas production sites, Environ. Sci. Technol., 2016, 50(9), 4877-4886, DOI:

490 10.1021/acs.est.6b00705.

Lyon, D. R., Zavala-Araiza, D., Alvarez, R. A., Harriss, R., Palacios, V., Lan, X., Talbot, R., Lavoie, T., Shepson, P., Yacovitch, T. I., and Herndon, S. C.: Constructing a spatially resolved methane emission inventory for the Barnett Shale region, Environ. Sci. Technol., 2015, 49(13), 8147-8157, DIO: 10.1021/es506359c.

Nathan, B. J., Golston, L. M., O'Brien, A. S., Ross, K., Harrison, W. A., Tao, L., Lary, D. J., Johnson, D. R., Covington, A.

495 N., Clark, N. N., and Zondlo, M. A.: Near-field characterization of methane emission variability from a compressor station using a model aircraft, Environ. Sci. Technol., 2015, 49(13), 7896-7903, DIO: 10.1021/acs.est.5b00705.

National Academies of Sciences, Engineering, and Medicine: Improving Characterization of Anthropogenic Methane Emissions in the United States, Washington, DC, The National Academies Press, 2018, DOI: 10.17226/24987.

Pernini, T.G., Zaccheo, T.S., Dobler, J., and Blume, N.: Estimating oil sands emissions using horizontal path-integrated column

500 measurements, Atmos. Meas. Tech., 2022. 15, 225-240, DOI: 10.5194/amt-15-225-2022.

Riddick, S. N., Ancona, R., Mbua, M., Bell, C. S., Duggan, A., Vaughn, T. L., Bennett, K., and Zimmerle, D. J.: A quantitative comparison of methods used to measure smaller methane emissions typically observed from superannuated oil and gas infrastructure, Atmos. Meas. Tech., 2022, 15(21), 6285-6296, DIO: 10.5194/amt-2022-9.

Sherwin, E.D., Chen, Y., Ravikumar, A.P., and Brandt, A.R.: Single-blind test of airplane-based hyperspectral methane detection via controlled releases, Elementa: Science of the Anthropocene, 2021, 9(1) DOI: 10.1525/elementa.2021.00063.

United States Environmental Protection Agency (EPA), Overview of Greenhouse Gases, 2022: https://www.epa.gov/ghgemissions/overview-greenhouse-gases, last access: 6 June 2023.

United States Environmental Protection Agency (EPA), Understanding Global Warming Potentials, 2023: https://www.epa.gov/ghgemissions/understanding-global-warming-potentials, last access: 6 June 2023.

Vaughn, T. L., Bell, C. S., Pickering, C. K., Schwietzke, S., Heath, G. A., Pétron, G., Zimmerle, D. J., Schnell, R. C., and Nummedal, D.: Temporal variability largely explains top-down/bottom-up difference in methane emission estimates from a natural gas production region, Proc. Natl. Acad. Sci. U.S.A., 2018, 115(46), 11712-11717, DIO: 10.1073/pnas.1805687115.

Watremez, X., Marble, A., Baron, T., Marcarian, X., Dubucq, D., Donnat, L., Cazes, L., Foucher, P.-Y., Dano, R., Elie, D., Chamberland, M., Gagnon, J.-P., Gay, L. B., Dobler, J., Ostrem, R., Russu, A., Schmidt, M., and Zaouak, O.: Remote sensing technologies for detecting, visualizing and quantifying gas leaks, Soc. Petrol. Eng. International Conference and Exhibition on Health, Safety, Security, Environment, and Social Responsibility, Abu Dhabi, UAE, 2018, DOI: 10.2118/190496-MS.

Zaccheo, T. S., Blume, N., Pernini, T., Dobler, J., and Lian, J.: Bias correction of long-path CO2 observations in a complex urban environment for carbon cycle model inter-comparison and data assimilation, Atmos. Meas. Tech., 2019. 12, 5791–5800, DOI: 10.5194/amt-12-5791-2019.

Zavala-Araiza, D., Lyon, D. R., Alvarez, R. A., Davis, K. J., Harriss, R., Herndon, S. C., Karion, A., Kort, E. A., Lamb, B. K., Lan, X., Marchese, A. J., Pacala, S. W., Robinson, A. L., Shepson, P. B., Sweeney, C., Talbot, R., Townsend-Small, A., Yacovitch, T. I., Zimmerle, D. J., and Hamburg, S. P.: Reconciling divergent estimates of oil and gas methane emissions, Proc. Natl. Acad. Sci. U.S.A., 2015, 112(51), 15597-15602, DIO: 10.1073/pnas.1522126112.